EAI Endorsed Transactions
on Context-aware Systems and Applications Research Article **EAI.EU**

Spatiotemporal lightmorphic computing for Carpathian roads

Dumitru Damian*

Information and Communication Engineering, Research and development consultant, Timișoara, 300003, Romania
Email: dumitrudamian@yahoo.com

Abstract

Energy consumption optimization by predicting vehicle behaviour in a dynamic environment represents an active research topic for the automotive industry. As vehicles are increasingly being equipped with driving assistance systems that function under dynamic driving conditions, a trajectory specific energy saving strategy must consider the trajectory particularities and predict in real time the opportunities for energy savings.

Researching and understanding the interactions between complex light intensity shapes and the trajectory spatiotemporal specificity is the main objective of the presented spatiotemporal lightmorphic computing framework for the Romanian Carpathian A1 and DN7 road network. Alternating start and stop locations are included, between the following major cities: București, Timișoara, Deva, Sibiu, Pitești.

Each trajectory segment measurement is composed from various slices defined as segmentation lengths (SL) that characterize the light signatures and trajectory profile. The light intensity variations are contained in the light distribution tensor Γ_t.

When analyzing the measured values, similarities between measurements are captured in a trajectory specific data-set Φ. This spatiotemporal light distribution symmetry is used to predict the trajectory unique virtual light shape evolution.

Observing the light intensity variations offers a unique perspective on the mentioned route. Having a framework to characterize the light signature structural patterns for specific road trajectories, helps to solve several real-world problems like: achieving optimal energy balance for specific trajectories or accurate estimation of light intensity phenomena that can impact the interaction between vehicle and traveling environment.

Received on 05 March 2021; accepted on 23 April 2021; published on 27 April 2021

Keywords: Carpathians, BH1750, framework, patterns, lightmorphic, Arduino, Spatiotemporal

doi:10.4108/eai.27-4-2021.169422

1. Introduction

Researching and understanding the interaction between complex light intensity morphing shapes and the traveled trajectories is the main objective of this work, with the aim at better characterizing the complex interactions between light availability and spatiotemporal specificity for the Romanian Carpathian road network formed by the A1-DN7 roads.

The basic idea is to extract the spatiotemporal lightmorphic profile from raw data by using a sensor sequence of values that are indexed in chronological order and have a structured nature, which is very common in many real-world applications. To that extent, a data collection methodology was established through a low-cost, small footprint sensor system [1] with data recording ability [2].

*Corresponding author. Email: dumitrudamian@yahoo.com

Various degrees of freedom(DoF) for the light virtual shapes are considered. The energy demand can be anticipated not only from the driver's perspective[3] but also from how the vehicle will react to its environment. Additionally by adding the trajectory specific light signature as a predictive feature of the energy management control system, it is possible to anticipate in real-time the trajectory specific energy savings potential.

By conducting the spatiotemporal lightmorphic computing for the acquired trajectory data, a unique virtual light signature is discovered. Next, by comparing historical trajectory data with the light distribution patterns, it is possible to predict the light morphing shape for certain trajectory segments.

2. Related research

With the developed framework to analyze the spatiotemporal lightmorphic shape for specific trajectories, new products and services can be derived.

Previous work to use light availability for specific trajectories include observing the vehicle swiveling headlamps and light intensity for particular highway geometric designs [4] or the effect of light intensity on flight trajectory in bumblebees [5].

Besides the energy aware engineered systems, the patterns in light intensity variation may be used to determine the light availability for roadside vegetation optimal growing conditions [6].

The selected trajectory is composed of the A1 highway and the national road DN7. Approximately 560km are covered in this research with multiple measurements for certain sections of the route. For the selected trajectory, various studies about the fauna [7], archaeological footprints or roadside geological vulnerability [8] exist.

3. Mathematical framework

The vehicle is considered to be a rigid body. As such it is possible to define in the XYZ coordinate system, a position vector for a point P that is located on the vehicle body, that will have the following vector representation:

$$\vec{r} = x_t * \vec{i} + y_t * \vec{j} + z_t * \vec{k}$$

The position vector for the next time-step is represented as:

$$\vec{r'} = x'_t * \vec{i'} + y'_t * \vec{j'} + z'_t * \vec{k'}$$

The dynamic relation between $\vec{r'}$ and $\vec{r}$ can be represented as:

$$i' = \alpha_{11} * i + \alpha_{12} * j + \alpha_{13} * k$$

$$j' = \alpha_{21} * i + \alpha_{22} * j + \alpha_{23} * k$$

$$k' = \alpha_{31} * i + \alpha_{32} * j + \alpha_{33} * k$$

A matrix that characterizes the vehicle position change for one time step will have the following representation:

$$C = \begin{pmatrix} \alpha_{11} & \alpha_{12} & \alpha_{13} \\ \alpha_{21} & \alpha_{22} & \alpha_{23} \\ \alpha_{31} & \alpha_{32} & \alpha_{33} \end{pmatrix}$$

Considering the sum of multiple sequential matrices, a vehicle position trajectory can be composed:

$$\Gamma = \sum_{i=1}^{\mathbb{N}} C_i \tag{1}$$

By observing the light intensity variations and the distribution of measurements, a trajectory specific light tensor can be defined as:

$$\Gamma_t = f(\Gamma_{IDT}) \tag{2}$$

where:

- I – intensity of light varies accordingly to seasons or weather conditions
- D – distribution characteristics for the same trajectory
- T – trajectory adjustments due to vehicle speed variations between departure and destination

For example, considering a predefined measurement segmentation length (SL) having the value of three, with two consecutive trajectory slices and three distributions, the light tensor can be derived as having the following representation:

$$\Gamma_{SL_1} = \begin{pmatrix} a_{111} & a_{121} & a_{131} \\ a_{211} & a_{221} & a_{231} \\ a_{311} & a_{321} & a_{331} \end{pmatrix}$$

$$\Gamma_{SL_2} = \begin{pmatrix} a_{112} & a_{122} & a_{132} \\ a_{212} & a_{222} & a_{232} \\ a_{312} & a_{322} & a_{332} \end{pmatrix}$$

The trajectory specific light tensor is constructed by using the three mode-n unfolding:

$$\Gamma_{(1)} = \begin{pmatrix} a_{111} & a_{121} & a_{131} & a_{112} & a_{122} & a_{132} \\ a_{211} & a_{221} & a_{231} & a_{212} & a_{222} & a_{232} \\ a_{311} & a_{321} & a_{331} & a_{312} & a_{322} & a_{332} \end{pmatrix}$$

$$\Gamma_{(2)} = \begin{pmatrix} a_{111} & a_{211} & a_{311} & a_{112} & a_{212} & a_{312} \\ a_{121} & a_{221} & a_{321} & a_{122} & a_{222} & a_{322} \\ a_{131} & a_{231} & a_{331} & a_{132} & a_{232} & a_{332} \end{pmatrix}$$

$$\Gamma_{(3)} = \begin{pmatrix} a_{111} & a_{211} & a_{311} & a_{121} & \dots & a_{231} & a_{331} \\ a_{112} & a_{212} & a_{312} & a_{122} & \dots & a_{232} & a_{332} \end{pmatrix}$$

The trajectory tensor values are considered to be included in the real numbers group, $\Gamma_t \in \mathbb{R}^{\prod_{i=1}^{\mathbb{N}} K_i}$ where:

- K_i – modes index for the trajectory tensor
- $\mathbb{R}$ – group of real numbers

A graphical representation with Matplotlib [9] of the trajectory specific light intensity tensor for five measurements and a predefined SL value is given in figure 1.

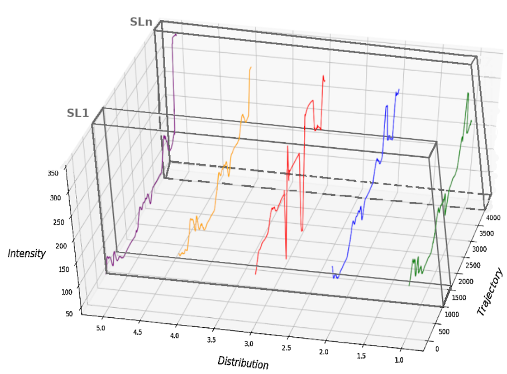

Figure 1. Predefined segment from the light intensity tensor

3.1. Probable light shape morphing

Values for the trajectory specific light tensor are captured in a data-set:

$$\Theta = \sum \Gamma_{IDT} \qquad (3)$$

While analyzing the data-set it is possible to discover similarities between segments of them $\{\Gamma^1_{IDT}, \Gamma^2_{IDT}, \dots, \Gamma^j_{IDT}\}$.
Values for the trajectory specific light tensor that show similarities are captured in a data-set:

$$\Phi_{\Gamma_{IDT}} = \sum_{j=1}^{\mathbb{N}} \Gamma^j_{IDT} \qquad (4)$$

While observing the distribution of multiple light segments within the data-set $\Phi_{\Gamma_{IDT}}$, it will be possible to estimate the probability for trajectory specific light tensor shape evolution:

$$p_\Phi = f(\rho_k p_{\Phi_k}) \qquad (5)$$

where:

- p_{Φ_k} – data-base k-th segment specific probability
- ρ_k – prediction weight for the k-th segment takes values from 0 to 1

The obtained probability shape for the similarities data-set, will be used as baseline homogenization characterization for the virtual light morphing shapes.

3.2. Spatiotemporal lightmorphic signature

For each specific trajectory, a unique spatiotemporal lightmorphic signature function can be defined as:

$$f_{L_\odot} = \int_1^I \int_1^D \int_1^T \Gamma_t \zeta_t dt \qquad (6)$$

where:

- Γ_t – trajectory tensor
- ζ_t – point in time specificity

Since the $f_{L_\odot}$ is continuous, the mean absolute error(MAE) between measured and estimated values can be considered.

$$MAE = \frac{1}{n} \sum_i^n \mid m_{\vec{f_{L_\odot}}} - e_{\vec{f_{L_\odot}}} \mid$$

where:

- n – number of samples for the considered trajectory
- $m_{\vec{f_{L_\odot}}}$ – light signature specific measured value
- $e_{\vec{f_{L_\odot}}}$ – light signature estimated value

3.3. Light vector field circulation

Since a point P is defined in the $\mathbb{R}^3$ space with the origin coordinates at $P = \{0; \vec{i}, \vec{j}, \vec{k}\}$, for multiple trajectory measurements, there is the opportunity to define a continuous light vector field $\bar{v}$ that describes the light morphing shape:

$$\bar{v}(x, y, z) = M(x, y, z)\vec{i} + N(x, y, z)\vec{j} + T(x, y, z)\vec{k} \qquad (7)$$

The vector field circulation for the unique light signature function $f_{L_\odot}$ can be characterized as:

$$\int_{f_{L_\odot}} \bar{v} d\bar{r} = \int_{f_{L_\odot}} [M(r(t)\dot{x}(t)) + N(r(t)\dot{y}(t)) + T(r(t)\dot{z}(t))]dt \tag{8}$$

4. Experimental considerations

Previous research in computational design explain how to convert a single input mesh into a parametric model by using methods such as cages [10], linear blend skinning [11] or manifold harmonics. Such methods can generate smooth virtual deformations for shapes that seem more organic in behavior.

While observing the measured data for light shape distribution on specific trajectories it was discovered that there are symmetry patterns in the light intensity distribution values.

From the saved data it is possible to randomly select various light intensity vector shapes. As indicated above in the spatiotemporal lightmorphic equation (6) each particular driving path will have unique light signatures that are used to generate smooth virtual light evolution shapes.

4.1. Hardware components

All the measurements are done using the same vehicle, driver and propulsion system.

Vehicle weight	m	1523	kg
ICE max. mech. power	$P_{ice-max}$	51	kW
Battery capacity	Q_0	55	Ah
Drivetrain	−−	FWD	−−
Transmission	−−	Manual	−−
Number of gears	−−	5	−−
Aerodynamic drag coefficient	C_x	0.33	−−
Front suspension	−−	Independent	−−
Low beam lights	−−	Halogen	*Active*

Table 1. Vehicle Parameters

In table 1, specific vehicle parameters are described. The sensor is placed on the windshield, inside the vehicle and facing outwards. As a result, the light intensity sensor will record the light variations due to the vehicle movement on the selected road trajectory, as it turns and bends following the road profile. Windshield tilt is not varied during the measurements. Only daytime sensor values are considered.

Data is recorded using Arduino UNO [2]. Light intensity is measured using the BH1750 [1] digital 16bit serial output type ambient light sensor.

The HW system is recording the data with same predefined recurrence for all the measurements. When analyzing the data, a median value is considered for every 100 measurements.

Measurements are done for trajectories that represent the Romanian Carpathian roads A1 and DN7, with alternating start and stop locations between the following major cities: București, Timișoara, Deva, Sibiu, Pitești. A map for the complete trajectory is drawn in figure 2.

Figure 2. Romanian Carpathians A1-DN7 light intensity measurement trajectory

4.2. Computing components

In order to analyze the measurement data, algorithms are written, that follow the equations defined in the mathematical framework.

Each trajectory can use various measurement slices defined as segmentation lengths (SL) to characterize the light signatures and trajectory profile.

For finding unique light signatures specific for each segment of trajectory, the algorithm for light signatures is used.

For finding matching light segments between measurements, the algorithm for light patterns is used.

Algorithm 1 Light Signatures

```
INPUT: Light measurements for the same trajectory
OUTPUT: Total segments and unique light signatures
BEGIN
    segmentation length (SL) ← value
    meas one ← light.data

    DEFINE the function light signature
            with the arguments (meas one, SL):
      FOR i ← 0 TO LEN(meas one) AND STEP(SL):
        RETURN:
            segmented data ← [SL]
      ENDFOR

    x ← 0
    light signatures ← []

    WHILE x < LEN(segmented data):
        current segment ← segmented data [x]
        x ← x + 1
        segment signs ← []
        FOR i,j ← ITERATOR
            current segment(value, next value):
          IF ← i = j
            APPEND segment signs ← " = "
          ELIF ← i < j
            APPEND segment signs ← " < "
          ELIF ← i > j
            APPEND segment signs ← " > "
        ENDFOR

        APPEND light signatures ← segment signs

    ENDWHILE

    unique light signatures ← []

        FOR elem ← light signatures
            APPEND unique light signatures ← [segment]
        ENDFOR

END
```

Algorithm 2 Light Patterns

```
INPUT: Measurements for the same trajectory
OUTPUT: Matching light segments
BEGIN
    index ← 0
    matched pattern ← 0

    FOR pattern ← meas two:
        index ← index + 1
        FOR signature ← meas one:
          WHILE LEN(pattern)< LEN(meas one):
            REMOVE ← meas one [SL]
            IF ← pattern = meas one [SL]
            matched pattern ← matched pattern +1
        ENDFOR
    ENDFOR

END
```

5. Obtained results

The complete Romanian Carpathians A1-DN7 spatiotemporal lightmorphic trajectory from București to Timișoara is analyzed.

From Deva to Timișoara a total of five measurements were considered, while for the trajectory segment Timișoara to Deva, two path variations of the same trajectory segment were considered. For path I, there were four measurements, while for path II there were three.

From Deva to Pitești via Sibiu there were three measurements considered, while for the trajectory segment Pitești to Deva via Sibiu there were two measurements considered.

For the Deva to București trajectory segment there was one measurement considered.

5.1. Deva to Timișoara trajectory segment

The specific light signature for the trajectory segment from Deva to Timișoara of highway A1 and DN7 roads is measured and analyzed.

The physical trajectory length is relatively constant while the journey duration varies between 3.5 and 5 hours.

As described in equation 2 the light intensity variations are forming the light distribution tensor Γ_t.

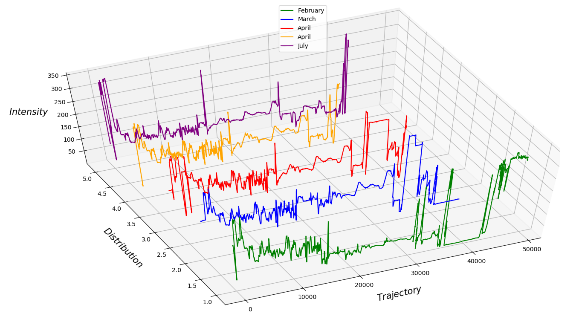

Figure 3. Measured light values for the trajectory segment Deva –> Timișoara of A1-DN7 road network

Five light intensity measurements are considered with the trajectory tensor having the following representation along the distribution dimension:

$$\Gamma_{t(DV \to TM)} = f(\Gamma_{I1T}, \Gamma_{I2T}, \Gamma_{I3T}, \Gamma_{I4T}, \Gamma_{I5T})$$

As described in equation 3 a specific data-set can be constructed:

$$\Theta_{(DV\rightarrow TM)} = \Gamma_{I1T} + \Gamma_{I2T} + \Gamma_{I3T} + \Gamma_{I4T} + \Gamma_{I5T}$$

From the data-set $\Theta_{(DV\rightarrow TM)}$ it can be observed that with an increasing SL, the unique light signatures and the trajectory light segments are converging towards each other.

After running the unique light signature algorithm, the results are saved in table 2.

Segmentation length	10	15	20	30
Γ_{I1T} trajectory segments	4880	3253	2440	1627
Γ_{I1T} light signatures	2152	2926	2379	1625
Γ_{I2T} trajectory segments	4500	3000	2250	1500
Γ_{I2T} light signatures	1863	2619	2192	1497
Γ_{I3T} trajectory segments	4073	2716	2037	1358
Γ_{I3T} light signatures	1439	2191	1934	1352
Γ_{I4T} trajectory segments	3484	2323	1742	1162
Γ_{I4T} light signatures	530	1601	1472	1105
Γ_{I5T} trajectory segments	4217	2811	2109	1406
Γ_{I5T} light signatures	1285	2418	2069	1404

Table 2. Number of light intensity segments and unique light signatures with various SL for trajectory segment Deva to Timișoara

Similarities between measurements are captured in a trajectory specific light signature data-set Φ as described in equation 4.

$$\Phi_{(DV\rightarrow TM)} = \sum_{j=1}^{5} \Gamma_{IDT}^{j}$$

For a predefined SL, after running the algorithm for light patterns between measurements, the results are saved in table 3.

SL = 30	Γ_{I1T}	Γ_{I2T}	Γ_{I3T}	Γ_{I4T}	Γ_{I5T}
Γ_{I1T}	—	103	134	2009	21
Γ_{I2T}	15	—	295	513	71
Γ_{I3T}	81	146	—	681	72
Γ_{I4T}	1447	150	235	—	41
Γ_{I5T}	18	58	81	545	—

Table 3. Non-unique matching light segments between measurements for trajectory segment Deva to Timișoara with SL=30

For a future light distribution Γ_{IXT}, each probable light segment has the corresponding prediction weight ρ_k. If there is a probable light segments match between distributions, the ρ_k will have a value of one. If there is not the ρ_k will have a value of zero.

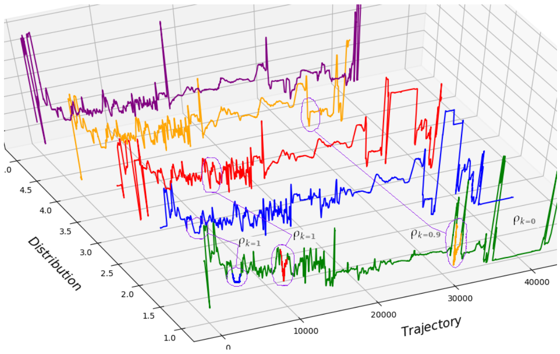

Figure 4. Specific ρ_k probability distribution based on Γ_{I1T} segments in the data-set Φ

Considering as baseline the first distribution Γ_{I1T} in the data-set Φ, a total of 2267 light segments are possible candidates for light segments matching with the other measured distributions $\Gamma_{I2T}, \Gamma_{I3T}, \Gamma_{I4T}, \Gamma_{I5T}$:

Thus a future distribution X that considers the Γ_{I1T} as baseline, will have the following probability value representation:

$$p_{\Phi_{\Gamma_{IXT}}} = f(\rho_k p_{\Phi_{\Gamma_{I2T_k}}}, \rho_k p_{\Phi_{\Gamma_{I3T_k}}}, \rho_k p_{\Phi_{\Gamma_{I4T_k}}}, \rho_k p_{\Phi_{\Gamma_{I5T_k}}}) \quad (9)$$

The baseline can change between any of the recorded distributions.

Analyzing the observed similarities between Γ_{I1T} and Γ_{I2T} leads to the discovery of a unique spatiotemporal lightmorphic shape as represented in figure 5:

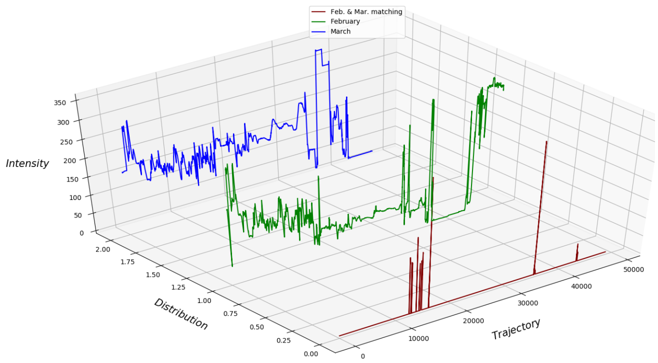

Figure 5. Unique light segments between Γ_{I1T} and Γ_{I2T} for SL=30 and $\rho_k \geq 0.7$

Repeating the same analysis, between Γ_{I1T} and Γ_{I3T} the unique light segments are represented in figure 6, between Γ_{I1T} and Γ_{I4T} the unique light segments are represented in figure 7 and between Γ_{I1T} and Γ_{I5T} the unique light segments are represented in figure 8.

According to spatiotemporal lightmorphic equation 6 a future distribution X that considers the Γ_{I1T} as

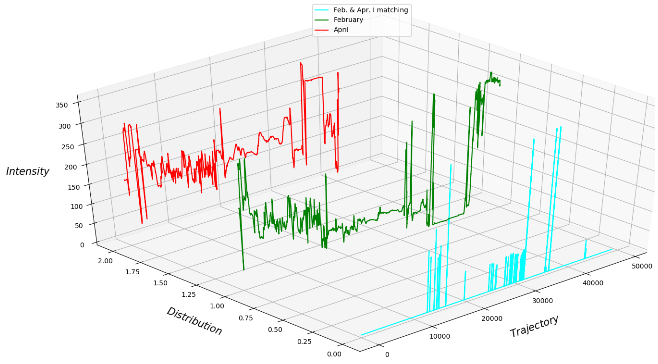

Figure 6. Unique light segments between Γ_{I1T} and Γ_{I3T} for SL=30 and $\rho_k \geq 0.7$

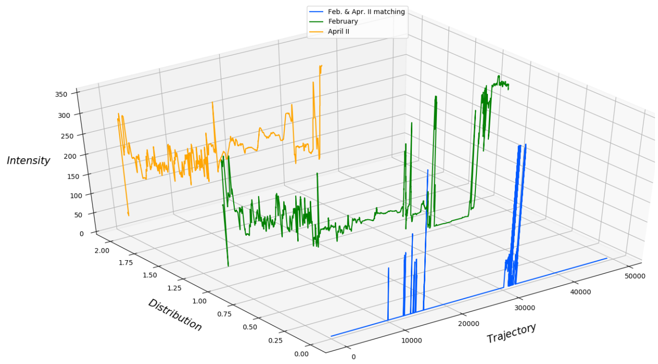

Figure 7. Unique light segments between Γ_{I1T} and Γ_{I4T} for SL=30 and $\rho_k \geq 0.7$

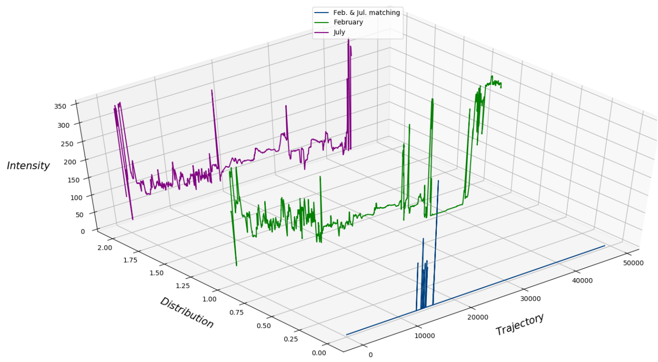

Figure 8. Unique light segments between Γ_{I1T} and Γ_{I5T} for SL=30 and $\rho_k \geq 0.7$

baseline will circulate between the virtual probable shapes as in figure 9.

The baseline distribution can change between any of the measured distributions ($\Gamma_{I1T}, \Gamma_{I2T}, \Gamma_{I3T}, \Gamma_{I4T}, \Gamma_{I5T}$).

With changing baseline between distributions Γ_{I1T},Γ_{I2T},Γ_{I3T},Γ_{I4T},Γ_{I5T} for $\rho_k \geq 0.7$, the virtual probable light shapes are represented in figure 10

According to equation 6 the unique light signature function for the trajectory Deva to Timișoara along the distribution dimension, can be represented as:

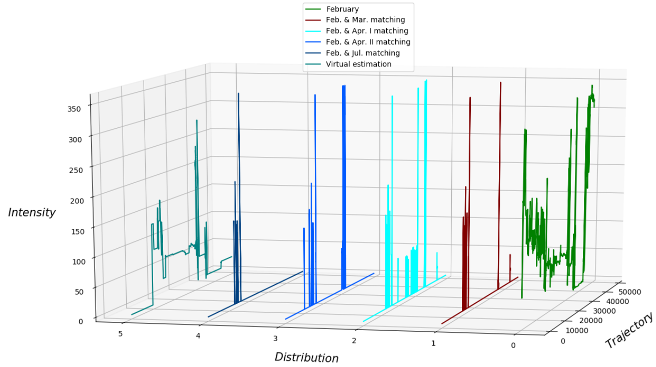

Figure 9. Virtual light distribution based on light segments matching with the baseline Γ_{I1T}

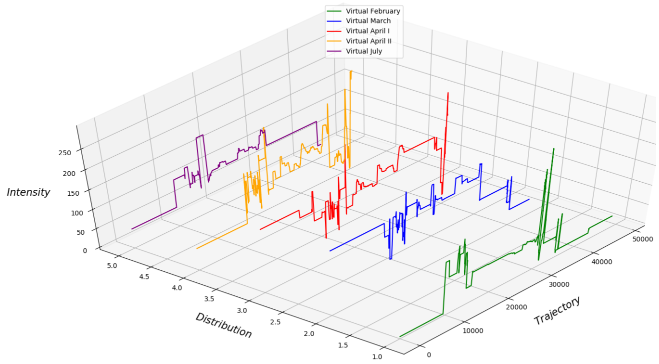

Figure 10. Virtual probable light signatures for trajectory Deva to Timișoara with SL=30 and $\rho_k \geq 0.7$

$$f_{L_{\odot(DV \to TM)}} = \int_{1}^{D} \Gamma_{t(DV \to TM)} \zeta_{t(DV \to TM)} dt$$

Following the same analysis, it is possible to add into consideration the variability for light intensity and specific trajectory characteristics as described in equation 6 and obtain a unique spatiotemporal lightmorphic shape.

$$f_{L_{\odot(DV \to TM)}} = \int_{1}^{I} \int_{1}^{D} \int_{1}^{T} \Gamma_{t(DV \to TM)} \zeta_{t(DV \to TM)} dt$$

5.2. Timișoara to Deva trajectory segment

The specific light signature for the trajectory from Timișoara to Deva segment of A1-DN7, is measured and analyzed in figure 11 and 13.

Trajectory length is relatively constant while the journey duration varies between 3.5 and 4.5 hours.

Four light intensity measurements are considered with the trajectory tensor having the following

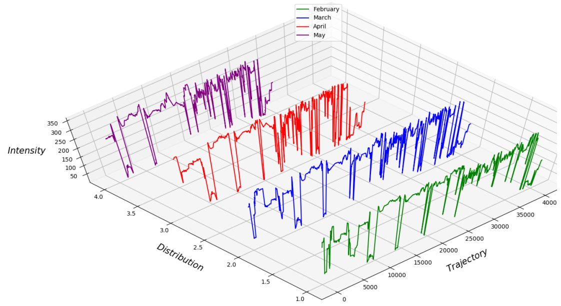

Figure 11. Measured light values for the Timișoara to Deva (path 1) segment of A1-DN7

representation:

$$\Gamma_{t_{(TM\rightarrow DV(I))}} = f(\Gamma_{I1T}, \Gamma_{t_{I2T}}, \Gamma_{t_{I3T}}, \Gamma_{t_{I4T}})$$

As considered in equation 3 a specific data-set is constructed:

$$\Theta_{(TM\rightarrow DV(I))} = \Gamma_{I1T} + \Gamma_{t_{I2T}} + \Gamma_{t_{I3T}} + \Gamma_{t_{I4T}}$$

From the data-set $\Theta_{(TM\rightarrow DV(I))}$ it can be observed how with an increasing SL, the unique light signatures and the trajectory light segments are converging towards each other.

After running the unique light signature algorithm, the results are saved in table 4.

Segmentation length	10	15	20	30
Γ_{I1T} trajectory segments	4072	2715	2036	1358
Γ_{I1T} light signatures	1446	2262	1945	1350
Γ_{I2T} trajectory segments	4065	2710	2033	1355
Γ_{I2T} light signatures	1465	2352	1994	1354
Γ_{I3T} trajectory segments	3401	2268	1701	1134
Γ_{I3T} light signatures	1102	1801	1592	1132
Γ_{I4T} trajectory segments	2977	1985	1489	993
Γ_{I4T} light signatures	1057	1581	1365	979

Table 4. Number of light intensity segments and unique light signatures with various segmentation lengths for Timișoara to Deva (I) trajectory

As considered in equation 4, similarities between measurements are captured in a trajectory specific data-set Φ .

$$\Phi_{(TM\rightarrow DV(I))} = \sum_{j=1}^{4} \Gamma_{IDT}^{j}$$

For a predefined SL, after considering the algorithm for matching light patterns between measurements, the results are saved in table 5.

SL = 30	Γ_{I1T}	Γ_{I2T}	Γ_{I3T}	Γ_{I4T}
Γ_{I1T}	—	110	224	257
Γ_{I2T}	209	—	57	58
Γ_{I3T}	236	41	—	239
Γ_{I4T}	345	67	173	—

Table 5. Non-unique matching light segments between measurements for trajectory (I) Timișoara to Deva with SL=30

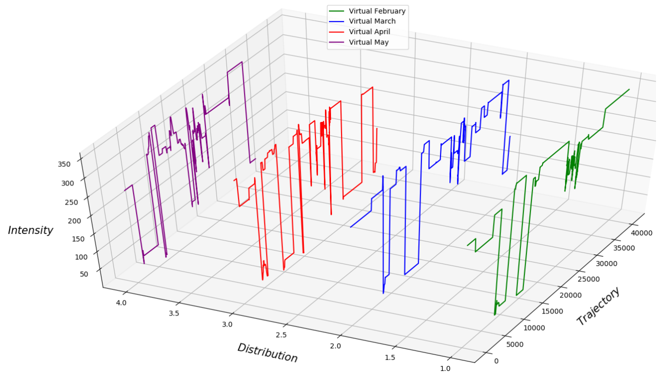

Figure 12. Virtual probable light signatures for trajectory (I) Timișoara to Deva with SL=30 and $\rho_k \geq 0.7$

With changing baseline between distributions Γ_{I1T},Γ_{I2T},Γ_{I3T},Γ_{I4T} for $\rho_k \geq 0.7$, the virtual probable light shapes are represented in figure 12

By selecting a different trajectory configuration between highway A1 and the DN1 roads, the specific light signature changes accordingly and is represented in figure 13.

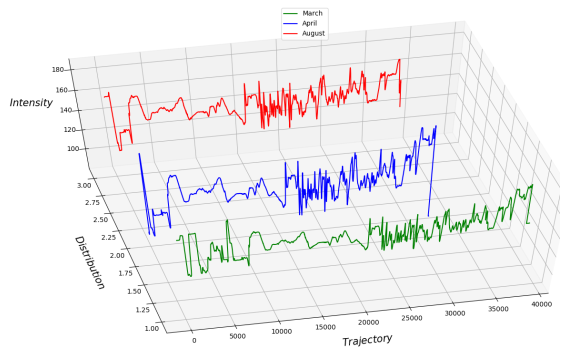

Figure 13. Measured light values for the Timișoara to Deva (path 2) segment of A1-DN7

Three light intensity measurements are considered with the trajectory tensor having the following representation:

$$\Gamma_{t_{(TM\rightarrow DV(II))}} = f(\Gamma_{I1T}, \Gamma_{t_{I2T}}, \Gamma_{t_{I3T}})$$

As previously, from the data-set $\Theta_{(TM\rightarrow DV(II))}$ it can be observed that with an increasing SL, the unique light signatures and the trajectory light segments are converging towards each other.

After running the unique light signature algorithm, the results are saved in table 6.

Segmentation length	10	15	20	30
Γ_{I1T} trajectory segments	3835	2557	1918	1279
Γ_{I1T} light signatures	1471	2183	1861	1275
Γ_{I2T} trajectory segments	3272	2181	1636	1091
Γ_{I2T} light signatures	1182	1883	1599	1088
Γ_{I3T} trajectory segments	3369	2246	1685	1123
Γ_{I3T} light signatures	1271	2027	1657	1122

Table 6. Number of light intensity segments and unique light signatures with various segmentation lengths for Timișoara to Deva trajectory (II)

Similarities between measurements are captured in a trajectory specific data-set Φ saved in table 7.

SL = 30	Γ_{I1T}	Γ_{I2T}	Γ_{I3T}
Γ_{I1T}	—	400	255
Γ_{I2T}	299	—	184
Γ_{I3T}	316	353	—

Table 7. Non-unique matching light segments between measurements for trajectory (II) Timișoara to Deva with SL=30

With changing baseline between distributions Γ_{I1T},Γ_{I2T},Γ_{I3T} for $\rho_k \geq 0.7$, the virtual probable light shapes are represented in figure 14.

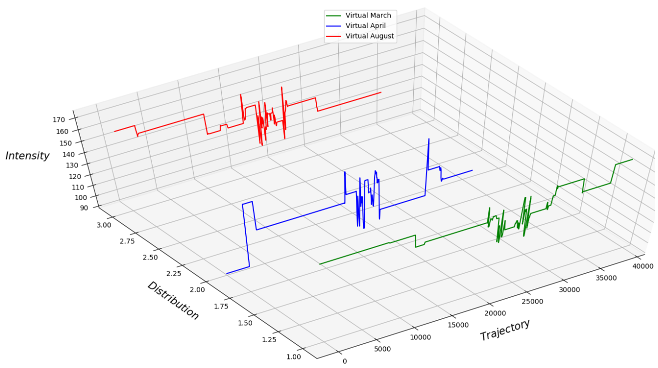

Figure 14. Virtual probable light signatures for trajectory (II) Timișoara to Deva with SL=30 and $\rho_k \geq 0.7$

5.3. Deva to Pitești (via Sibiu) trajectory segment

The specific light signature for the trajectory from Deva to Pitești (via Sibiu) segment of A1-DN7, is measured and analyzed.

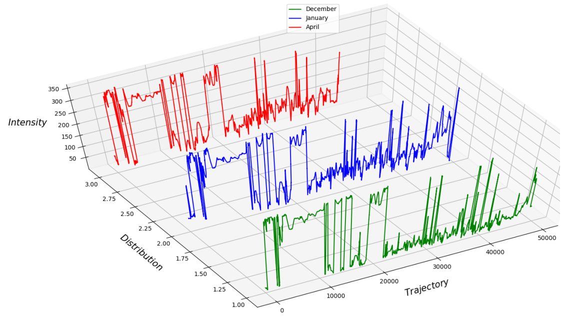

Figure 15. Measured light values for the Deva to Pitești (via Sibiu) segment of A1-DN7

Three light intensity measurements are considered with the trajectory tensor having the following representation:

$$\Gamma_{t(DV \to AG)} = f(\Gamma_{I1T}, \Gamma_{t_{I2T}}, \Gamma_{t_{I3T}})$$

As described in equation 3 a specific data-set is constructed for the indicated trajectory:

$$\Theta_{(DV \to AG)} = \Gamma_{I1T} + \Gamma_{t_{I2T}} + \Gamma_{t_{I3T}}$$

From the data-set $\Theta_{(DV \to AG)}$ it can be observed how with an increasing SL, the unique light signatures and the trajectory light segments are converging towards each other.

After running the unique light signature algorithm, the results are saved in table 8.

Segmentation length	10	15	20	30
Γ_{I1T} trajectory segments	4939	3293	2470	1647
Γ_{I1T} light signatures	1607	3056	2461	1647
Γ_{I2T} trajectory segments	4928	3286	2464	1643
Γ_{I2T} light signatures	1624	3007	2447	1643
Γ_{I3T} trajectory segments	4238	2826	2119	1413
Γ_{I3T} light signatures	1111	2261	2031	1413

Table 8. Number of light intensity segments and unique light signatures with various segmentation lengths for Deva to Pitești (via Sibiu) trajectory

Similarities between measurements are captured in a trajectory specific data-set $\Phi_{(DV \to AG)}$ as described in equation 4.

The selected predefined SL is 20 segments and after considering the algorithm for matching light patterns between measurements, the results are saved in table 9.

With changing baseline between distributions Γ_{I1T},Γ_{I2T},Γ_{I3T} for $\rho_k \geq 0.7$, the virtual probable light shapes are represented in figure 16.

SL = 20	Γ_{I1T}	Γ_{I2T}	Γ_{I3T}
Γ_{I1T}	—	637	610
Γ_{I2T}	568	—	1047
Γ_{I3T}	605	1151	—

Table 9. Non-unique matching light segments between measurements for trajectory Deva to Sibiu to Pitești with SL=20

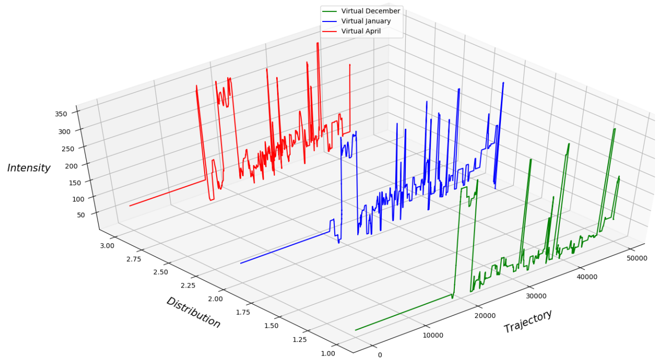

Figure 16. Virtual probable light signatures for trajectory segment Deva to Pitești (via Sibiu) with SL=20 and $\rho_k \geq 0.7$

5.4. Pitești to Deva (via Sibiu) trajectory segment

The specific light signature for the trajectory from Pitești to Deva (via Sibiu) segment of A1-DN7, is measured and analyzed.

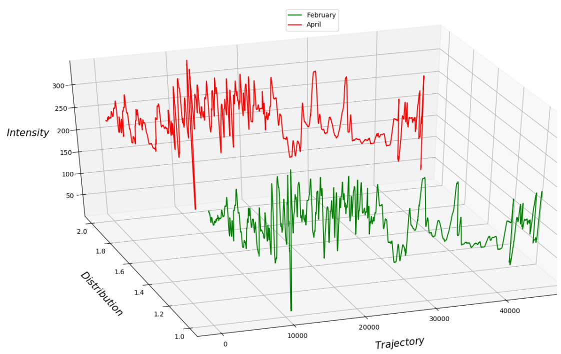

Figure 17. Measured light values for the Pitești to Deva (via Sibiu) segment of A1-DN7

Two light intensity measurements are considered with the trajectory tensor having the following representation:

$$\Gamma_{t_{(AG \to DV)}} = f(\Gamma_{I1T}, \Gamma_{I2T})$$

From the data-set $\Theta_{(AG \to DV)}$ it can be observed how with an increasing SL, the unique light signatures and the trajectory light segments are converging towards each other.

After running the unique light signature algorithm, the results are saved in table 10.

Segmentation length	10	15	20	30
Γ_{I1T} trajectory segments	4536	3024	2268	1512
Γ_{I1T} light signatures	1200	2443	2178	1505
Γ_{I2T} trajectory segments	4601	3068	2301	1534
Γ_{I2T} light signatures	1160	2369	2141	1522

Table 10. Number of light intensity segments and unique light signatures with various segmentation lengths for Pitești to Deva (via Sibiu) trajectory

The selected predefined SL is 20 segments and after considering the algorithm for matching light patterns between measurements, the results are saved in table 11.

SL = 20	Γ_{I1T}	Γ_{I2T}
Γ_{I1T}	...	5812
Γ_{I2T}	5906	...

Table 11. Non-unique matching light segments between measurements for trajectory Pitești to Deva (via Sibiu) with SL=20

With changing baseline between distributions Γ_{I1T},Γ_{I2T} for $\rho_k \geq 0.7$, the virtual probable light shapes are represented in figure 18.

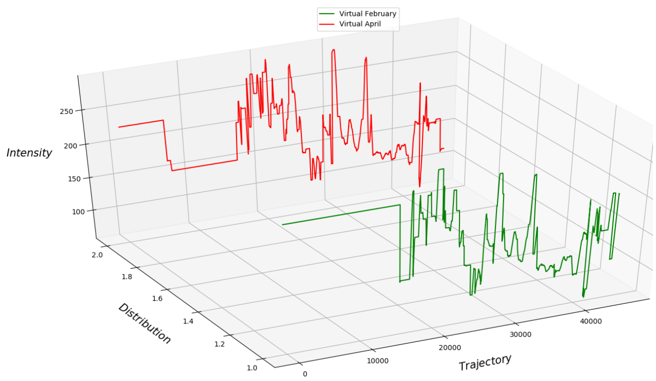

Figure 18. Virtual probable light signatures for trajectory segment Pitești to Deva (via Sibiu) with SL=20 and $\rho_k \geq 0.7$

5.5. Deva to București trajectory segment

The specific light signature for the trajectory from Deva to București segment of A1-DN7, is measured and analyzed.

One light intensity measurement is available with the trajectory tensor having the following representation:

$$\Gamma_{t_{(DV \to B)}} = f(\Gamma_{I1T})$$

After running the unique light signature algorithm, the results are saved in table 12.

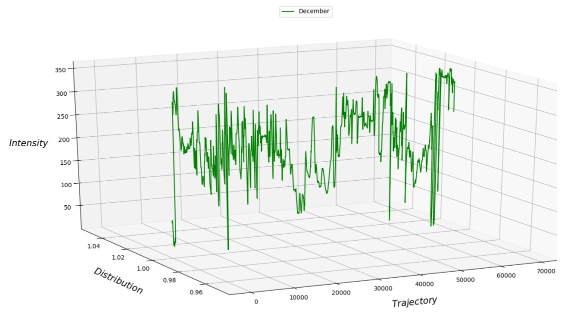

Figure 19. Measured light values for the Deva to București (via Sibiu) segment of A1-DN7

Segmentation length	10	15	20	30
Γ_{I1T} trajectory segments	7781	5187	3891	2594
Γ_{I1T} light signatures	2453	4631	3840	2592

Table 12. Number of light intensity segments and unique light signatures with various segmentation lengths for Deva to București (via Sibiu) trajectory

Analyzing the unique light signature function for the trajectory Deva to București along the measured distribution, multiple virtual light signature shapes can be derived as represented in figure 20.

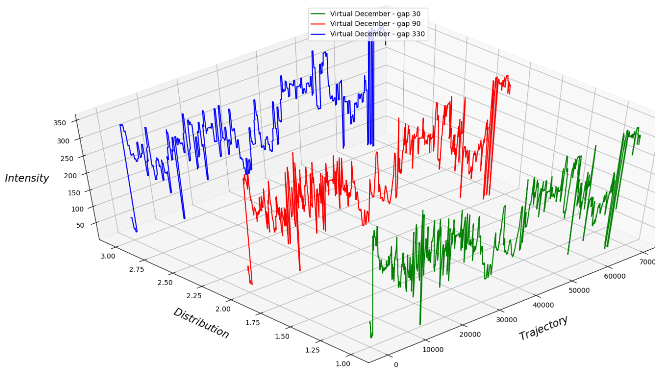

Figure 20. Virtual probable light signatures for trajectory segment Deva to București with SL=30

In order to obtain the derived virtual shapes, isochronous data gaps are artificially created. The spatiotemporal lightmorphic computing framework is able to accommodate such data gaps and provide an estimated virtual shape.

6. Conclusion

The method developed in this work is designed to provide a framework for other research efforts to use the spatiotemporal lightmorphic computing in other various energy saving projects.

The method is applied to the Romanian Carpathian A1 and DN7 road network in order to obtain virtual light shapes and determine the optimum energy saving driving strategies.

Several questions have been answered trough the analysis and usage of the spatiotemporal lightmorphic computing framework:

- Can the optimum vehicle reaction be predicted for the selected trajectory when the light signature is estimated.
- What will be the optimum energy saving driving style for the predicted trajectory considering dynamic vehicle external parameters.
- What shape will the unique light signature have for the Romanian Carpathian A1 and DN7 road network.
- Is it possible to estimate the light signature for future driving scenarios.

Additional sensor measurements are planned to be added in the existing light intensity data-base like: sound characteristics, specific vibrations, unique humidity variations, temperature profile, chemical components concentration levels.

With this sensor fusion approach, the optimum energy conservation configurations can be discovered for specific trajectories.

Having this evolution of knowledge, a better understanding of the light intensity specificity for the Romanian Carpathian A1 and DN7 road network might lead to innovative vehicles and smart infrastructures.

References

[1] BH1750, https://learn.adafruit.com/adafruit-bh1750-ambient-light-sensor. Accessed: 2021-01-23.

[2] Arduino UNO, https://www.arduino.cc/en/Guide/ArduinoUno. Accessed: 2021-01-23.

[3] Coiret, A., Deljanin, E. and Vandanjon, P.O. (2020) Vehicle energy savings by optimizing road speed-sectioning. *European Transport Research Review* **12**(41). URL https://doi.org/10.1186/s12544-020-00432-8.

[4] De Santos-Berbel, C. and Castro, M. (2020) Effect of vehicle swiveling headlamps and highway geometric design on nighttime sight distance. *Mathematics and Computers in Simulation* **170**: 32 – 50. doi:https://doi.org/10.1016/j.matcom.2019.08.012.

[5] Reber, T., Vähäkainu, A., Baird, E., Weckström, M., Warrant, E. and Dacke, M. (2015) Effect of light intensity on flight control and temporal properties of photoreceptors in bumblebees. *Journal of Experimental Biology* **218**(9): 1339–1346. doi:10.1242/jeb.113886, URL https://jeb.biologists.org/content/218/9/1339. https://jeb.biologists.org/content/218/9/1339.full.pdf.

[6] Yasin, M., Rosenqvist, E., Jensen, S.M. and Andreasen, C. (2019) The importance of reduced light intensity on the growth and development of six weed species. *Weed Research* **59**(2): 130–144. doi:https://doi.org/10.1111/wre.12352, URL https://onlinelibrary.wiley.com/doi/abs/10.1111/wre.12352. https://onlinelibrary.wiley.com/doi/pdf/10.1111/wre.12352.

[7] Rosca, S., Simonca, V., Bilasco, S., Vescan, I., Fodorean, I. and Petrea, D. (2019) The assessment of favourability and spatio-temporal dynamics of pinus mugo in the romanian carpathians using gis technology and landsat images. *Sustainability* **11**(13). doi:10.3390/su11133678, URL https://www.mdpi.com/2071-1050/11/13/3678.

[8] Ovreiu, A., Bărsoianu, I., Nistor, C., Nedelea, A. and Comănescu, L. (2019) Assessment of vulnerability for rockfalls in cozia gorge (southern carpathians, romania. *Natural Hazards* **99**(117–140). URL https://doi.org/10.1007/s11069-019-03732-y.

[9] Hunter, J.D. (2007) Matplotlib: A 2d graphics environment. *Computing in Science & Engineering* **9**(3): 90–95. doi:10.1109/MCSE.2007.55.

[10] Zheng, Y., Fu, H., Cohen-Or, D., Au, O.K.C. and Tai, C.L. (2011) Component-wise controllers for structure-preserving shape manipulation. *Computer Graphics Forum* **30**(2): 563–572. doi:https://doi.org/10.1111/j.1467-8659.2011.01880.x.

[11] Jacobson, A., Baran, I., Popović, J. and Sorkine, O. (2011) Bounded biharmonic weights for real-time deformation. *ACM Trans. Graph.* **30**(4). URL https://doi.org/10.1145/2010324.1964973.